The International Journal of Advanced Manufacturing Technology (2024) 132:893–906
https://doi.org/10.1007/s00170-024-13428-8

ORIGINAL ARTICLE

High-pressure die casting process optimization for improving shrinkage porosity and air entrainment in carburetor housing with aluminum alloy using Taguchi-based ProCAST simulation and MADM-based overall quality index

Ryong-Chol Kim[1] · Kyong-Ryul Hong[1] · Ji-Yon Yang[1] · Won-Chol Yang[1]

Received: 26 December 2023 / Accepted: 9 March 2024 / Published online: 19 March 2024

Abstract
Many practical high-pressure die casting process (HPDCP) optimization problems are multi-objective optimization ones that optimize multiple quality attributes of castings, simultaneously. This paper proposed a new HPDCP optimization method for improving volume of shrinkage porosity (VSP) and air entrainment (AE) using Taguchi-based ProCAST simulation and multi-attribute decision-making (MADM)-based overall quality index. Taguchi orthogonal array was used to design ProCAST simulation experiment. MADM was used to convert multiple quality attributes into a single overall quality index (OQI). Taguchi optimization method was used to determine the optimal HPDCP parameters to maximize the OQI. By using the proposed method, this paper determined the optimal HPDCP parameters such as pouring temperature (PT), filling rate in shot sleeve (FR), piston velocity (PV) and preheating mold temperature (PMT) for improving the VSP and AE in carburetor housing with aluminum alloy AlSi9Cu1Mg. The optimal HPDCP parameters were PT of 640 °C, FR of 40%, PV of 6.5 m/s, and PMT of 150 °C. The PT was the most effective HPDCP parameter for improving the VSP and AE, and the next were FR, PV, and PMT. The proposed method could be actively applied to not only HPDCP but also other casting processes and other manufacturing processes.

Keywords High-pressure die casting process (HPDCP) · Multi-attribute decision-making (MADM) · Process optimization · Taguchi method · ProCAST

1 Introduction

High-pressure die casting process (HPDCP) is one of well-known popular manufacturing processes for light metals such as aluminum (Al) alloys because of its high productivity, high dimensional accuracy, and excellent mechanical properties [1]. The HPDCP has been widely used to manufacture various products with high dimensional accuracy and productivities and has much faster production rate compared with other manufacturing methods. All major Al alloy automotive components would be manufactured with the HPDCP technology [2]. It is widely used to manufacture mass-produced metallic parts with complex shapes and precise dimensions [3]. It is widely used as a casting process for Al alloys, and about two-thirds of all Al alloy castings are used in automotive industry [4]. The pressure die casting is a manufacturing process in the non-ferrous industries producing engineered Al alloy products such as car components [5].

Die castings have usual gas porosity caused by gas in molten metal and air entrainment because the molten metal is filled in the die cavity at high velocity. In addition, they include shrinkage porosity due to unreasonable gating condition in the HPDCP. As a result, the internal porosity has significant influence on the quality of castings. There are several parameters in the HPDCP technology, and the quality of the die casting can be improved when controlling reasonably them. In the HPDCP, the controlling parameters are pouring temperature, mold temperature, filling rate in shot sleeve, piston velocity, injection pressure, and holding pressure. In order to determine the reasonable HPDCP parameters, the

✉ Won-Chol Yang
ywch71912@star-co.net.kp

[1] Faculty of Materials Science and Technology, Kim Chaek University of Technology, Pyongyang, Democratic People's Republic of Korea

numerical simulation has been widely introduced. Due to the fierce turbulence and limited shrinkage feeding capability, the defects such as entrapped air and shrinkage porosity may form in the castings and affect the stability of the mechanical properties of the castings. The main reasons of such variation in the mechanical properties of Al alloys come to randomness in distribution of the defects of castings, and it may cause the inhomogeneity in the cast microstructure and leads to early failure during the material deformation process. [1]

Carburetor housing is one of parts of internal combustion engine and it is manufactured by HPDCP. Therefore, the numerical HPDCP simulation of the carburetor housing has to be performed, and it is necessary to determine optimal process such as pouring temperature, filling rate in shot sleeve, piston velocity and die temperature using ProCAST, which is a software that can simulate the flow process of the molten metal in the shot sleeve, die cavity of the horizontal cold chamber HPDC machine and predict the position and volume of the shrinkage porosity and air entrainment in the die castings.

To determine reasonable casting process parameters for improving the shrinkage porosity and air entrainment in the die castings with a little amount of labor, time, and funds, it is necessary to conduct the simulation experiment using Taguchi experimental design method during ProCAST simulation work. Syrcos optimized the die casting process by determining optimal piston velocities at first and second stages, metal temperature, filling time, and hydraulic pressure for improving the density of AlSi9Cu3 Al alloy castings by Taguchi method [6]. Hsu et al. determined the pouring temperature, die temperature, piston velocities and multiplied pressure for automobile starter motor casting made from Al ADC10 by using L_{27} orthogonal array of Taguchi method [2]. Hu et al. determined the reasonable process parameters for die mold design of an A356 Al alloy polishing plate by using simulations, orthogonal experiments, and die casting experiment [7]. Tsoukalas determined the optimal die casting process parameters such as holding furnace temperature, die temperature, the 1st and 2nd stage plunger velocities, and the 3rd stage multiplied pressure for minimizing porosity of AlSi9Cu3 Al alloy die castings using Taguchi method, multiple linear regression, and genetic algorithm (GA) [3]. Verran et al. determined the optimal process parameters (slow shot, fast shot, and setup pressure) for improving the density of Al alloy die castings by Taguchi method [8]. Kittur et al. optimized the pressure die casting process parameters such as injection pressure, fast-shot velocity, phase-changeover point and holding time for improving the porosity, surface roughness, and hardness using desirability function approach [9]. Mohiuddin et al. optimized the process parameters for improving the density, ultimate tensile strength, and percentage elongation for Al7SiMg alloy castings using Taguchi method [10]. Apparao and Birru optimized five die casting process parameters such as injection pressure, molten metal temperature, plunger velocities at first and second stages, and die temperature for improving the density of A380 alloy casting using quality function deployment and Taguchi method [11]. Murugarajan and Raghunayagan optimized the pressure die casting process parameters such as injection pressure, shot velocity, and furnace temperature for improving micro-hardness and surface roughness of A413 Al alloy castings using central composite design, multiple regression analysis and desirability function approach [12].

Dou et al. proposed a novel optimization method for mechanical properties of Al alloy in HPDCP by combining experiment and modeling. They developed a finite element model for the entire HPDCP and determined the optimal piston slow shot profile by modeling the free surface wave evolution in the shot sleeve [1]. Dou et al. simulated the entire HPDCP of Al-Si alloy using the casting simulation package ProCAST and determined the optimal thermal die cycling and optimal piston profile [13]. Yan et al. performed the numerical simulation of AZ91D magnesium alloy automobile plug casting in the HPDCP and predicted the position of the shrinkage and slack of the die casting [14]. Sharifi et al. quantitatively studied the influences of the slow and fast stage velocities, intensification pressure, and die temperature on the amount of various defects such as shrinkage and gas porosity in the HPDC magnesium alloy components using ProCAST [15]. Boydak et al. investigated the mold filling, solidification, temperature distribution, porosity, and velocity of the molten metal during the HPDCP for Al alloy AlSi12Cu flange part through the computer simulation, and obtained the optimal parameters from the simulation results [16]. Fiorese et al. conducted the computational analysis and experimental assessment of the effect of the plunger speed on the tensile properties in HPDC using the software MAGMASOFT [17]. Armillotta et al. performed the HPDCP simulation of zinc alloys in order to reveal the occurrence of cold flow defects and found that the temperature at the end of the mold fill was important [18]. Korti and Abboudi discovered that the air entrainment caused by the molten metal flow in the slow stage of the HPDCP in the horizontal cold chamber had an influence on the porosity defect of the die castings [19]. Hu et al. showed that smoothed particle hydrodynamics (SPH) modeling for simulating HPDCP of A356 Al alloy polishing plate had high reliance in studying the flow state of the molten metal during mold cavity filling [20]. Jiang et al. investigated the effects of the casting process parameters such as gas flow rate, vacuum level and gas pressure on the internal quality (density and porosity of castings) of A356 castings by numerical simulation in the expendable pattern shell casting [21]. They described that the gas flow rate largely affected the filling ability and internal quality of A356 castings, and the optimal process

improved the filling ability, internal quality, microstructure, and surface quality of casting [22]. Yang et al. developed overall quality index and overall quality map according to the tensile mechanical properties and artificial aging heat treatment conditions for cast Al alloy using multi-attribute decision-making (MADM) and multiple regression analysis [23]. Yang et al. proposed a multi-attribute optimization methodology for the casting process optimization using Taguchi method and integrated MADM combined with some MADMs [24].

The previous works considered the shrinkage porosity and density as quality attributes of die castings and did not consider the air entrainment in the die castings, while the air entrainment in die castings often appears and it may produce the rejection of castings in practice. Therefore, it is necessary to consider not only the shrinkage porosity and density but also air entrainment in die castings.

On the other hand, although the previous works optimized the die casting process using Taguchi method, the works optimized the individual quality attribute such as porosity and density, respectively. The works did not optimize the multiple quality attributes simultaneously. It resulted in inconsistent optimal process parameters according to the individual quality attributes. Therefore, it is very important to develop an effective method to optimize multiple quality attributes of die castings simultaneously, not individually.

To do this, this paper proposed HPDCP optimization method for simultaneous improving the shrinkage porosity and air entrainment using Taguchi-based ProCAST simulation and MADM-based overall quality index (OQI). By using the proposed method, this paper determined the optimal HPDCP parameters such as pouring temperature, filling rate, piston velocity and preheating mold temperature for simultaneously improving the shrinkage porosity and air entrainment in carburetor housing with Al alloy AlSi9Cu1Mg.

2 Materials and methods

2.1 Materials

The chemical composition of Al alloy AlSi9Cu1Mg used for this work is shown in Table 1.

2.2 Three-dimensional (3D) model of carburetor housing for ProCAST simulation

Figure 1 shows three-dimensional (3D) model of the carburetor housing for ProCAST simulation.

As shown in Fig. 1, the size of the carburetor housing has a height of 135.5 mm and inner core with type of T letter. Its weight may be about 450 g. In addition, its outside has comparatively complex shape and average wall thickness of 3.5 mm.

2.3 Design method of ProCAST simulation experiment

For ProCAST simulation experiment, four high-pressure die casting process (HPDCP) parameters such as pouring temperature (PT), filling rate in shot sleeve (FR), piston velocity

Table 1 The chemical composition of Al alloy used for experiment

Element	Si	Fe	Cu	Mn	Mg	Ni	Zn	Al
wt%	8.5 ~ 9.5	1.2	0.8 ~ 1.2	0.5	0.35 ~ 0.45	0.3	0.2	Remainder

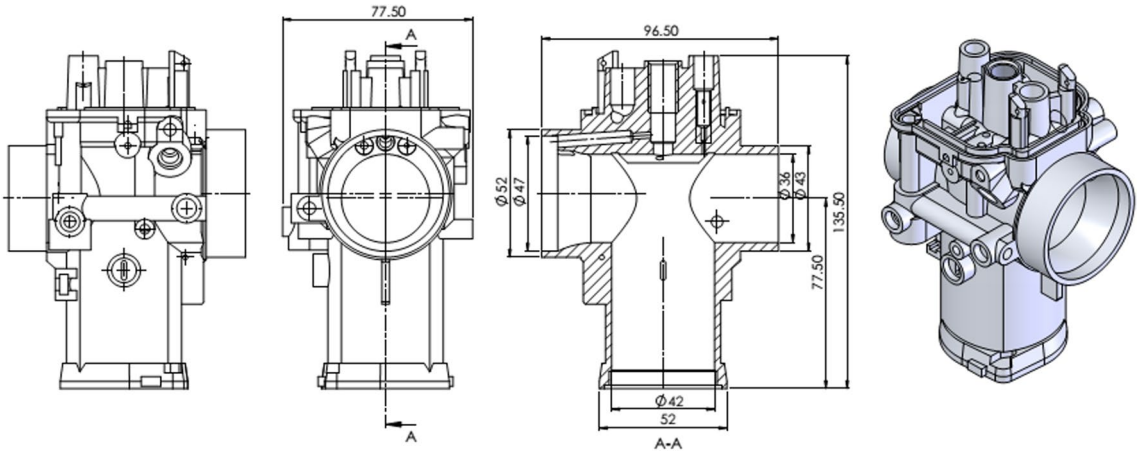

Fig. 1 Three-dimensional (3D) model of carburetor housing

(PV), and preheating mold temperature (PMT) were selected as the main controllable parameters, and other parameters were kept to constant values. For evaluating the quality of castings, two quality attributes (responses) such as volume of shrinkage porosity (VSP) and air entrainment (AE) were used.

Table 2 shows the controllable HPDCP parameters and their levels for simulation experiment.

As the number of HPDCP parameters is 4 and the number of levels is 3, Taguchi orthogonal array $L_9(3^4)$ was selected for design of simulation experiment. Table 3 shows Taguchi orthogonal array $L_9(3^4)$.

Four HPDCP parameters were respectively assigned to each column of $L_9(3^4)$.

Table 4 shows the experimental arrangement according to $L_9(3^4)$.

2.4 High-pressure die casting (HPDC) simulation method using ProCAST

The molten metal was freely poured in shot sleeve and then was filled the sleeve by piston motion at low velocity during the HPDCP. Next, the die cavity was filled with the molten metal by piston motion at high velocity. Therefore, the HPDCP simulation should include the main parameters such as pouring of molten metal, filling rate in shot sleeve, and piston velocity at slow and fast stages.

At first carburetor housing casting, fixed and mobile die, shot sleeve, and piston were designed using CAE software (Solidworks). At this time, the diameter of piston should be a bit greater than one of the shot sleeve. Then the size of element mesh of carburetor housing, die and shot sleeve, and piston was determined as 2 mm, 8 mm, and 5 mm, respectively. The material of carburetor housing was selected as EN AC-46400 AlSi9Cu1Mg of Al alloy in database of ProCAST software. The interface heat transfer coefficient between casting and mold was set by 900 W/m^2·K. The outer walls of mold and shot sleeve were cooled by air and the piston velocity at low stage was set by 0.8 m/s based on the technical characteristic of horizontal cold chamber high-pressure die casting machine.

In order to analyze the amount of air entrainment, the gas model was active and switched on by 1. For modeling of piston motion in the HPDCP, the algorithm of inter-penetration meshes was switched on. WALLF for computing the velocity of the free surface at the wall of die cavity was set by 0.99.

Table 2 HPDCP parameters and their levels

Levels	PT (°C)	FR (%)	PV (m/s)	PMT (°C)
1	640	40	2.5	150
2	670	50	4.5	200
3	700	60	6.5	250

Table 3 Taguchi orthogonal array $L_9(3^4)$

Trial no	1	2	3	4
1	1	1	1	1
2	1	2	2	2
3	1	3	3	3
4	2	1	2	3
5	2	2	3	1
6	2	3	1	2
7	3	1	3	2
8	3	2	1	3
9	3	3	2	1

2.5 Method to determine optimal HPDCP parameters using MADM and Taguchi method

The details of the method to determine optimal HPDCP parameters using MADM and Taguchi method are as follows:

Step 1: Conduct the ProCAST simulation at every experimental trials in Table 3, and evaluate the values of VSP and AE.

Let x_{ij} and y_{ik} be the values of *j-th* HPDCP parameter and *k-th* quality attribute (response) at *i-th* experimental trial ($i = \overline{1,9}, j = \overline{1,4}, k = \overline{1,2}$), respectively. Namely, x_{i1} is the value of PT, x_{i2} is the value of FR, x_{i3} is the value of PV and x_{i4} is the value of PMT for ProCAST simulation at *i-th* experimental trial, and y_{i1} is the evaluation value of VSP, and y_{i2} is the evaluation value of AE obtained from ProCAST simulation at *i*-th experimental trial.

The values of HPDCP parameters at every experimental trials constitute a HPDCP parameter matrix $= \left(x_{ij}\right)_{9\times4}$, and the values of VSP and AE constitute a decision matrix (DM) $Y = \left(y_{ik}\right)_{9\times2}$.

Step 2: Calculate MADM-based overall quality index (OQI) values at every experimental trials using MADM.

Table 4 Experimental arrangement according to $L_9(3^4)$

Trial no	HPDCP parameters			
	PT (°C)	FR (%)	PV (m/s)	PMT (°C)
1	640	40	2.5	150
2	640	50	4.5	200
3	640	60	6.5	250
4	670	40	4.5	250
5	670	50	6.5	150
6	670	60	2.5	200
7	700	40	6.5	200
8	700	50	2.5	250
9	700	60	4.5	150

The MADM is used to convert multiple quality attributes into a single OQI. To do this, some well-known MADM methods such as SAW, TOPSIS, GRA, and RSR are applicable [25, 26].

2–1: Constitute a normalized DM $Z = \left(z_{ik}\right)_{9\times2}$ from the DM $Y = \left(y_{ik}\right)_{9\times2}$.

The normalization of the DM converts all the attribute values into non-dimensional values. It transforms different units and scales of different attributes into common units and scales, and it allows the comparisons across the different attributes.

The normalization of DM was performed using the following linear min–max normalization formula ($i = \overline{1,9}, k = \overline{1,2}$):

$$z_{ik} = \left(y_{k\max} - y_{ik}\right) / \left(y_{k\max} - y_{k\min}\right), \tag{1}$$

where $y_{k\max}$ and $y_{k\min}$ are the maximum and minimum values of k-th quality attribute, respectively.

2–2: Constitute a weighted normalized DM $U = (u_{ik})_{9\times2}$.

The element u_{ik} is calculated as follows ($i = \overline{1,9}, k = \overline{1,2}$):

$$u_{ik} = w_k \bullet z_{ik}, \tag{2}$$

where w_1 and w_2 are the importance weights of VSP and AE, respectively. In this work, the importance weights of VSP and AE were set as $w_1 = 0.8$ and $w_2 = 0.2$ from the practical experience and knowledge.

2–3: Calculate the MADM-based OQI values (OQIs) $V_1,\ldots, V_i,\ldots, V_9$ at every experimental trials using the MADM method.

The MADM-based OQIs consist of the simple weighted sum values in SAW, the relative closeness values in TOPSIS method, the gray relational degrees in GRA method, and the rank sum ratio values in RSR method. The details of SAW, TOPSIS and GRA were described in Refs. [25, 26]. The MADM-based OQIs comprehensively reflect the multiple quality attributes at every experimental trials. The MADM-based OQI belongs to [0, 1], and the higher the value is, the better the quality of the casting is.

When some MADMs are used to calculate the OQIs, the final OQIs are introduced by combining the OQIs obtained from different MADMs.

Let $V_{m1}, V_{mi},\ldots, V_{m9}$ be the OQIs at every experimental trials using m-th MADM, $r_{m1}, r_{mi},\ldots, r_{m9}$ be the OQI ranks ($m = \overline{1,M}$). M is the number of the used MADMs. When 4 MADMs such as SAW, TOPSIS, GRA and RSR are used, M is 4.

The MADMs-based final OQI is determined using the priority weighted mean values of OQIs obtained from different MADMs. The final OQIs are calculated using the following formula ($i = \overline{1,9}$) [27]:

$$V_i = \sum_{m=1}^{M} \lambda_m \bullet V_{mi}, \tag{3}$$

where $\lambda_m; m = \overline{1,M}$ are the priority weights of the MADMs.

The priority weights are calculated by normalizing the mean values of the rank correlation coefficients as follows:

$$\lambda_m = \overline{\rho}_m / \sum_{k=1}^{M} \overline{\rho}_m, \tag{4}$$

where $\overline{\rho}_m$ is the mean value of Spearman's rank correlation coefficients between the OQIs using m-th MADM and other MADMs. It is calculated as follows:

$$\overline{\rho}_m = \frac{1}{M-1} \sum_{k=1,k\neq m}^{M} \rho_{mk} = \frac{1}{M-1} \sum_{k=1,k\neq m}^{M} \left[1 - \frac{6}{n\left(n^2-1\right)} \sum_{i=1}^{n} \left(r_{mi} - r_{ki}\right)^2\right]. \tag{5}$$

The larger the value is, the more the OQI ranks obtained from the corresponding MCDM are similar to the OQI ranks obtained from the other MCDMs.

The final OQI V_i represents the comprehensive quality of the castings in full consideration of the OQI values obtained from different MADMs and the priority weights of each MADM.

The MADM-based final OQIs are also called OQIs using combined MADM.

Step 3: Calculate the mean OQIs $\left\{S_{lj}; j = \overline{1,4}, l = \overline{1,3}\right\}$ of the HPDCP parameters at each level.

S_{lj} is the mean OQI of j-th HPDCP parameter at the l-th level.

Step 4: Calculate the ranges of mean OQIs of each HPDCP parameter.

The ranges of mean OQIs are calculated as difference between maximum OQI and minimum OQI as follows:

$$R_j = \max_{1\le l\le3}\left\{S_{lj}\right\} - \min_{1\le l\le3}\left\{S_{lj}\right\}. \tag{6}$$

The range of mean OQI R_j represents the influence of the j-th HPDCP parameter. The higher the value is, the higher the influence of the parameter is.

Step 5: Determine the optimal HPDCP parameter values to maximize the OQI.

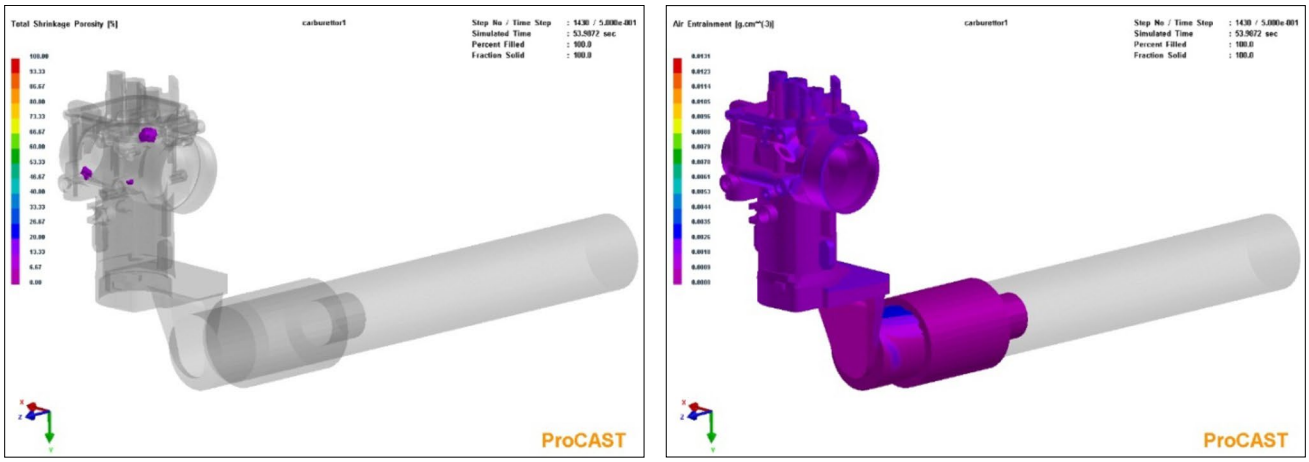

(a)

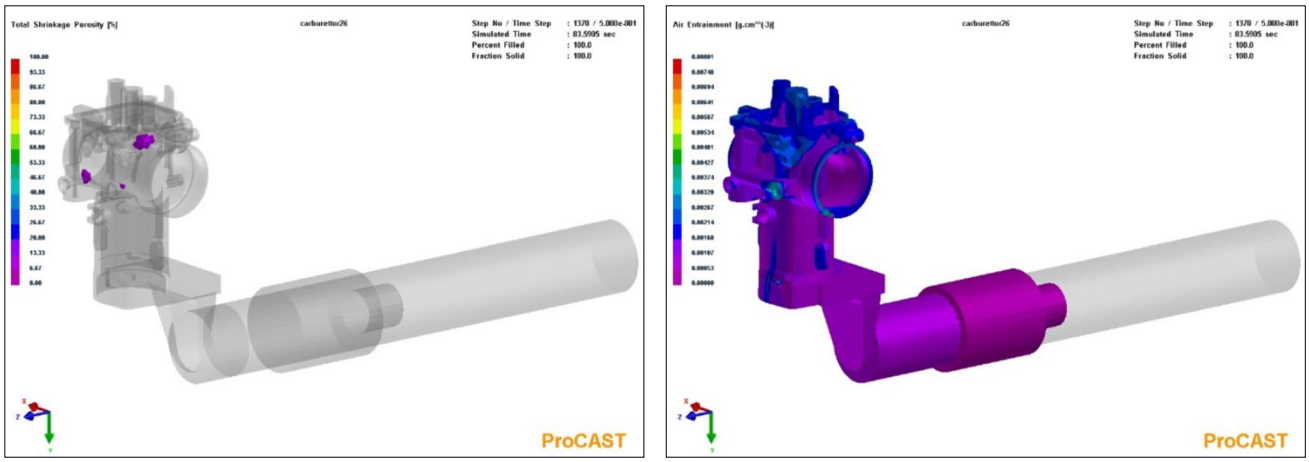

(b)

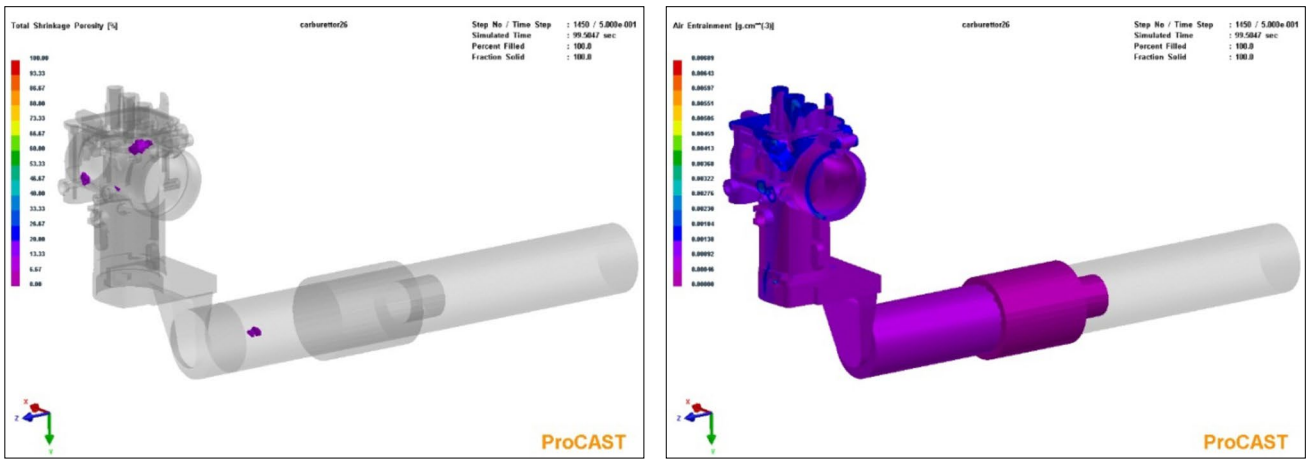

(c)

Fig. 2 Simulation experiment results using ProCAST at nine experimental trials: **a** trial no. 1, **b** trial no. 2, **c** trial no. 3, **d** trial no. 4, **e** trial no. 5, **f** trial no. 6, **g** trial no. 7, **h** trial no. 8, and **i** trial no. 9 (left: VSP, right: AE)

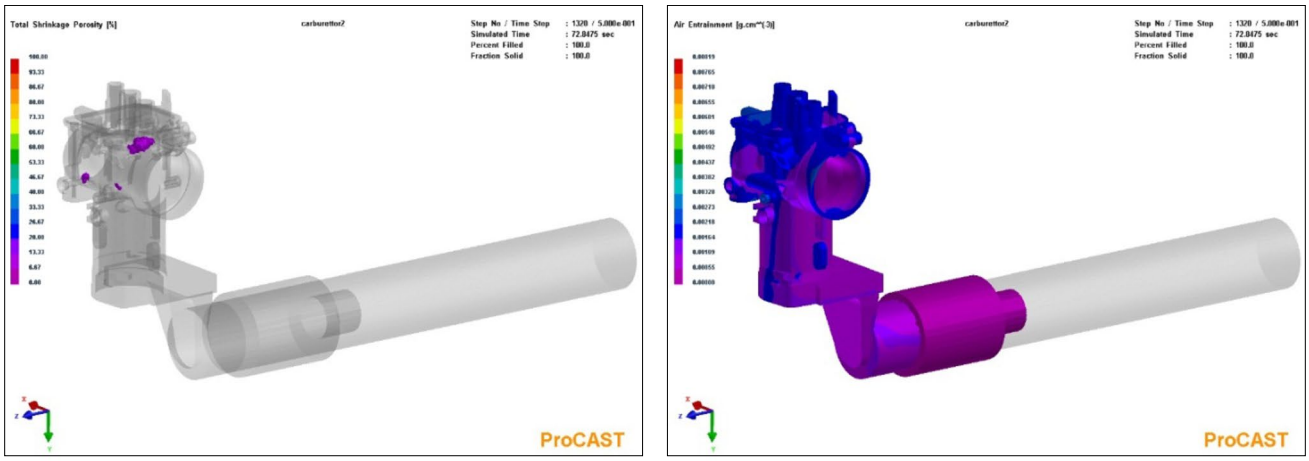

(d)

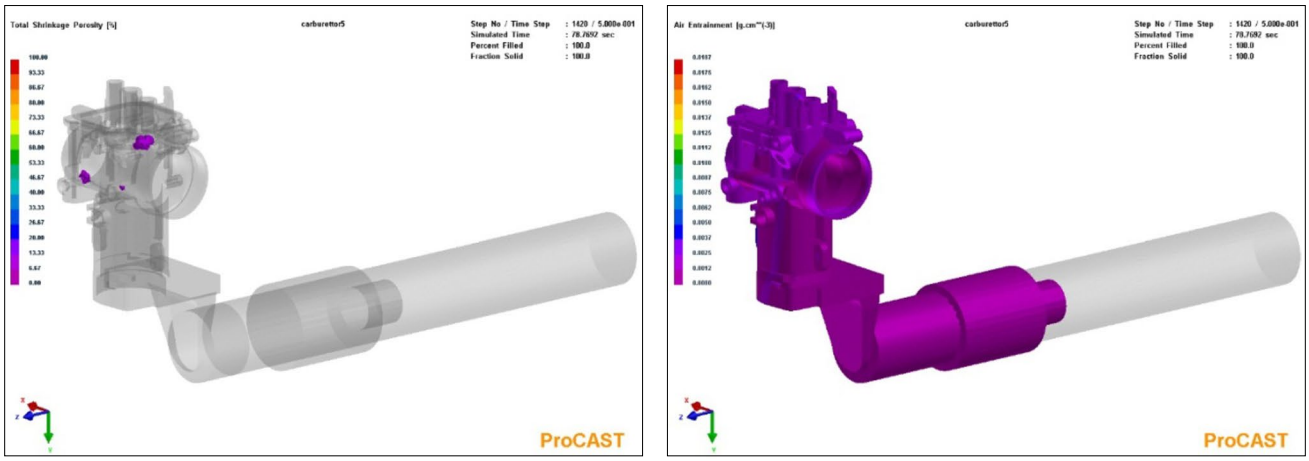

(e)

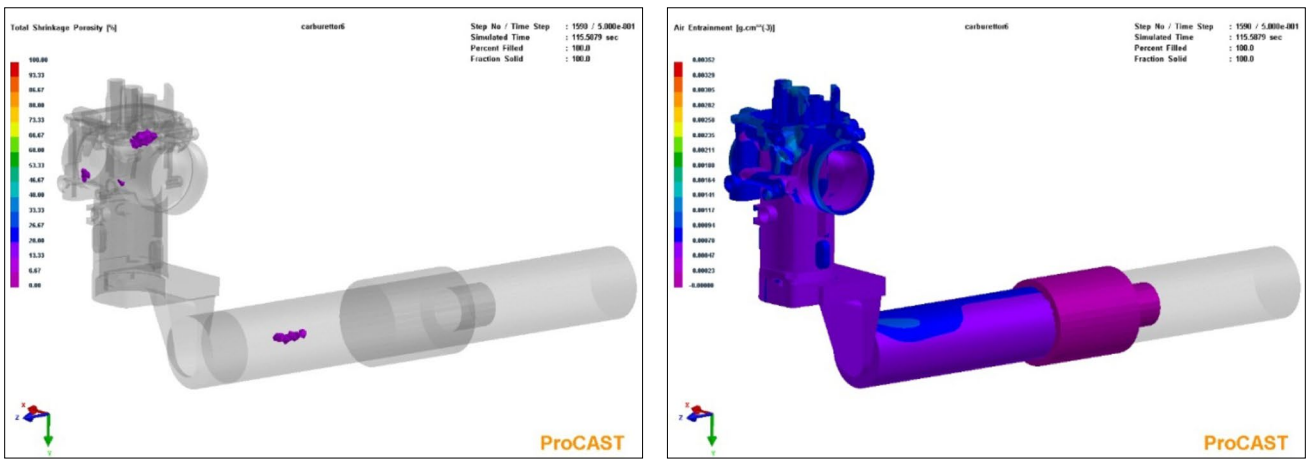

(f)

Fig. 2 (continued)

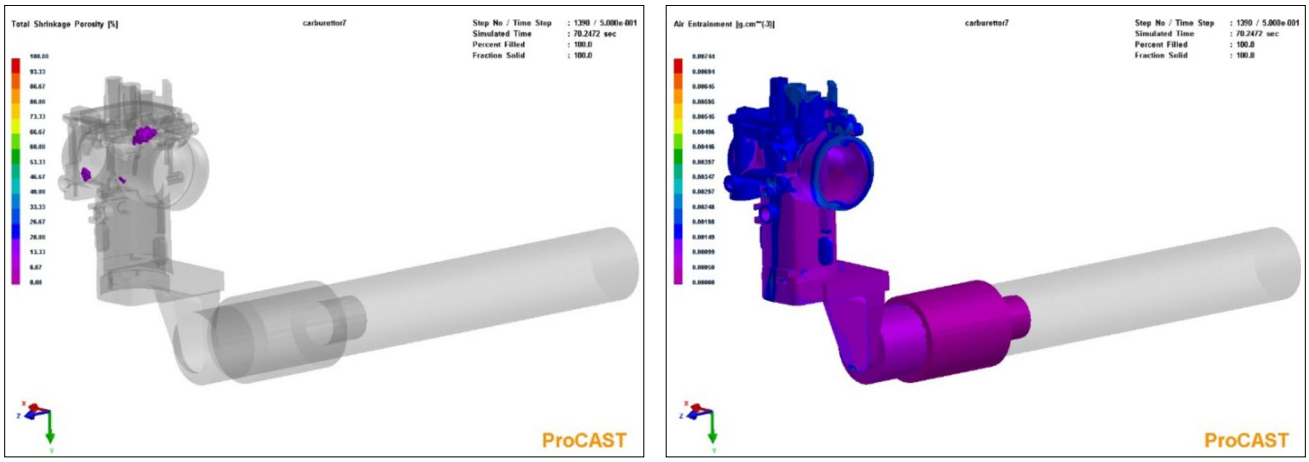

(g)

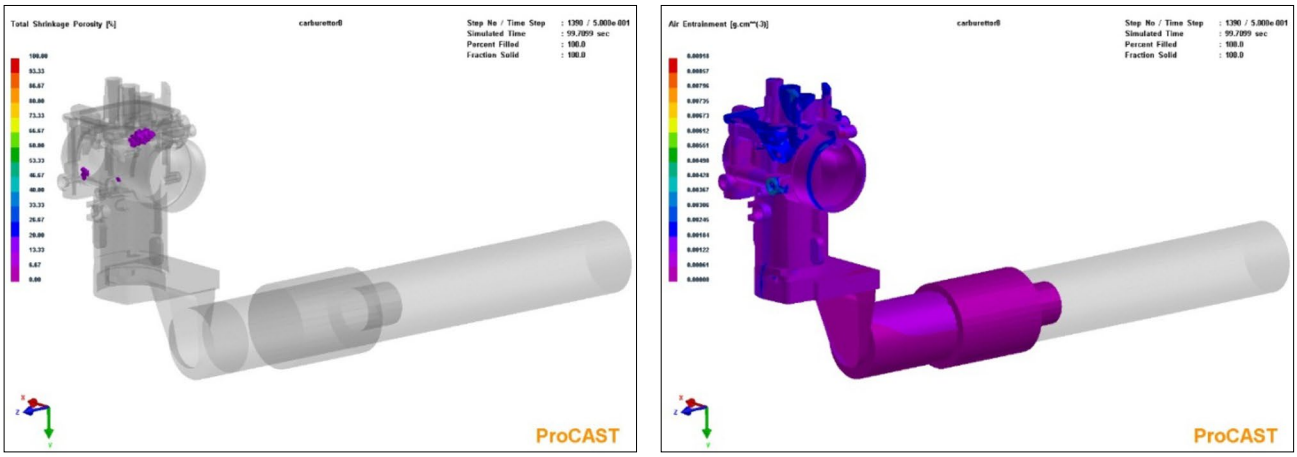

(h)

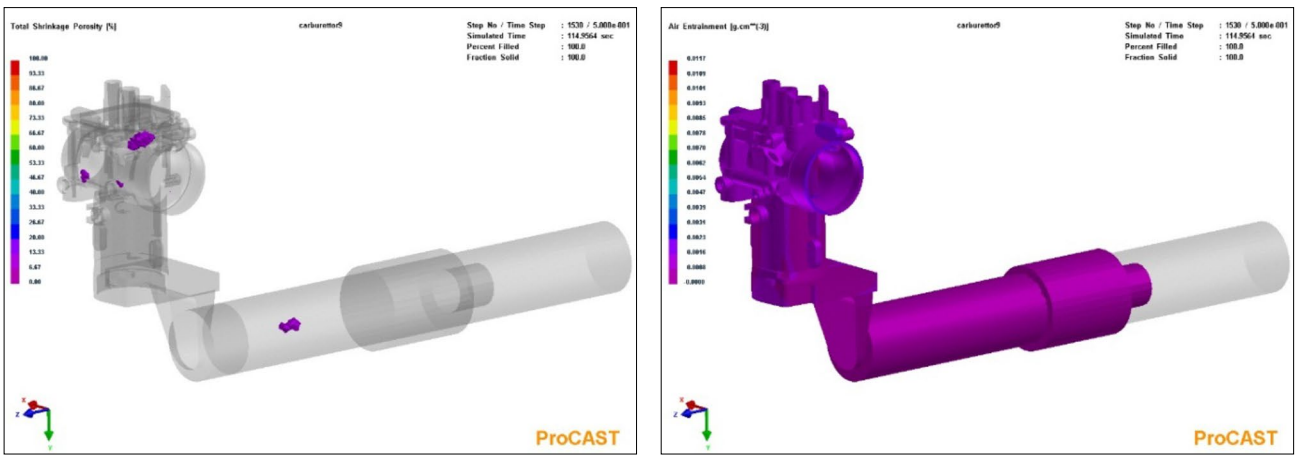

(i)

Fig. 2 (continued)

Table 5 Simulation experiment result values according to $L_9(3^4)$

Trial no	HPDCP parameters				Responses	
	PT (°C)	FR (%)	PV (m/s)	PMT (°C)	VSP (cm^3)	AE (g/cm^3)
1	640	40	2.5	150	0.219505	0.001375
2	640	50	4.5	200	0.270404	0.001420
3	640	60	6.5	250	0.320834	0.001037
4	670	40	4.5	250	0.356488	0.001450
5	670	50	6.5	150	0.283652	0.001361
6	670	60	2.5	200	0.542853	0.000767
7	700	40	6.5	200	0.337115	0.001454
8	700	50	2.5	250	0.421927	0.001225
9	700	60	4.5	150	0.566143	0.000953

Table 6 Normalized DM

Trial no	VSP	AE
1	1.000	0.115
2	0.853	0.049
3	0.708	0.607
4	0.605	0.006
5	0.815	0.135
6	0.067	1.000
7	0.661	0.000
8	0.416	0.333
9	0.000	0.729

Step 5–1: Determine the optimal level-combination H consisted of the levels to maximize the mean OQIs.

$$H = \left\{ \left(h_1, h_2, h_3, h_4\right) \middle| S_{h_j j} = \max_{1 \le l \le 3} \left\{ S_{lj} \right\}; j = \overline{1,4} \right\}. \quad (7)$$

Step 5–2: Determine the optimal HPDCP parameter values x_1*, x_2*, x_3*, x_4*, where x_j* is the parameter value corresponding to h_j-th level of j-th HPDCP parameter.

3 Results and discussion

Figure 2 shows the simulation results using ProCAST at nine experimental trials in Table 3.

In Fig. 2, the positions of shrinkage porosity in the casting were almost similar at every trials according to different values of PT, FR, PV, and PMT, but the VSPs and AEs were varied. As can be seen in Fig. 2, the more the pouring mass of the molten metal increases, the more the solidified amount in the shot sleeve increases. Therefore, the final position of the piston was far away from the casting, and the shrinkage porosity was identified in the solidified part of the shot sleeve (see the left subfigures in Fig. 2c, f, i). The influence of the piston pressure on the casting may be weak due to the increasement of pouring mass of the molten metal. When whole of the casting is purple colored, it indicates that the AE may be less (see the right subfigures in Fig. 2e, i), and when the casting contains some blue colored parts, it indicates that the AE may be more and more (see the right subfigures in Fig. 2b–d, f–h).

Table 5 shows the simulation experiment result values according to Taguchi orthogonal array $L_9(3^4)$. At every

Table 7 OQIs of nine experimental trials using 4 MADMs and combined MADM

Trial no	Orthogonal array				OQIs				Final OQIs
	PT	FR	PV	PMT	SAW	TOPSIS	GRA	RSR	Combined MADM
1	1	1	1	1	0.823	0.819	0.872	0.889	0.851
2	1	2	2	2	0.692	0.753	0.687	0.778	0.728
3	1	3	3	3	0.688	0.701	0.617	0.689	0.674
4	2	1	2	3	0.485	0.564	0.514	0.400	0.491
5	2	2	3	1	0.679	0.741	0.657	0.733	0.703
6	2	3	1	2	0.254	0.217	0.479	0.378	0.331
7	3	1	3	2	0.529	0.611	0.543	0.467	0.538
8	3	2	1	3	0.400	0.411	0.455	0.400	0.416
9	3	3	2	1	0.146	0.154	0.396	0.267	0.240

Table 8 Mean OQIs of the HPDCP parameters at three levels and their ranges using individual MADMs

MADMs	Levels	HPDCP parameters			
		PT	FR	PV	PMT
SAW	Level 1	0.734	0.612	0.492	0.549
	Level 2	0.473	0.590	0.441	0.492
	Level 3	0.358	0.362	0.632	0.524
	Ranges	0.376	0.250	0.191	0.058
	Range rates (%)	43.037	28.567	21.797	6.599
	Range ranks	1	2	3	4
	Optimal levels	1	1	3	1
TOPSIS	Level 1	0.758	0.665	0.482	0.571
	Level 2	0.508	0.635	0.491	0.527
	Level 3	0.392	0.357	0.684	0.559
	Ranges	0.366	0.307	0.202	0.044
	Range rates (%)	39.803	33.412	21.962	4.823
	Range ranks	1	2	3	4
	Optimal levels	1	1	3	1
GRA	Level 1	0.725	0.643	0.602	0.642
	Level 2	0.550	0.600	0.533	0.570
	Level 3	0.465	0.497	0.606	0.528
	Ranges	0.261	0.146	0.073	0.113
	Range rates (%)	43.955	24.554	12.353	19.138
	Range ranks	1	2	4	3
	Optimal levels	1	1	3	1
RSR	Level 1	0.785	0.585	0.556	0.630
	Level 2	0.504	0.637	0.481	0.541
	Level 3	0.378	0.444	0.630	0.496
	Ranges	0.407	0.193	0.148	0.133
	Range rates (%)	46.218	21.849	16.807	15.126
	Range ranks	1	2	3	4
	Optimal levels	1	2	3	1

Table 9 Mean OQIs of the HPDCP parameters at three levels and their ranges using combined MADM

Levels	HPDCP parameters			
	PT	FR	PV	PMT
Level 1	0.751	0.626	0.533	0.598
Level 2	0.508	0.616	0.486	0.532
Level 3	0.398	0.415	0.638	0.527
Ranges	0.353	0.211	0.152	0.071
Range rates (%)	44.842	26.867	19.288	9.003
Range ranks	1	2	3	4
Optimal levels	1	1	3	1

trials, the VSPs and AEs were calculated on Cutoff Info panel in ProCAST.

To convert two responses into single OQI, the 4 well-known MADMs such as SAW, TOPSIS, GRA, and RSR methods were used, where the last two columns corresponding to two responses (VSP and AE) in Table 5 constituted the DM.

Table 6 shows the normalized DM. Table 7 shows the OQIs of nine experimental trials using 4 MADMs and combined MADM.

In calculating the final OQIs combined with 4 MADMs, the priority weights of the MADMs were, respectively, 0.250, 0.253, 0.249, and 0.249.

Table 8 shows the mean OQIs of the HPDCP parameters at three levels and their ranges using SAW, TOPSIS, GRA, and RSR. Table 9 shows the mean OQIs of the HPDCP parameters at three levels and their ranges using combined MADM. Figure 3 shows the mean OQIs of the HPDCP parameters at three levels using combined MADM.

As can be seen from Table 9, the ranking of the influences of the HPDCP parameters is as follows:

$$PT(44.842\%) > FR(26.867\%) > PV(19.288\%) > PMT(9.003\%)$$

As shown in the ranking of the influences, the PT has the highest influence on the overall quality of the casting. According to the PT, its fluidity and shrinkage may be varied, and it becomes very important in the HPDCP. The FR and PV affect the air elimination in the shot sleeve and die cavity. The lower the FR is and the faster the PV is, the more the AE may increase. As the AE is also important quality attribute in the HPDCP, the FR and PV become the subsequent factors. On the other hand, although the PMT has a lower influence than the PT, FR and PV on the overall quality of the casting, it may decrease the thermal impact of the molten metal on die and ensure the fluidity of the molten metal.

From Table 9 and Fig. 3, we can find that the optimal levels of the HPDCP parameters are PT at the 1st level, FR at the 1st level, PV at the 3rd level, and PMT at the 1st level, and the optimal level-combination is as follows:

$$PT_1FR_1PV_3PMT_1.$$

Therefore, the optimal values of the HPDCP parameters are as follows:

$$\mathrm{PT}: 640^{\circ}\mathrm{C}, \mathrm{FR}: 40\%, \mathrm{PV}: 6.5\mathrm{m/s}, \mathrm{PMT}: 150^{\circ}\mathrm{C}.$$

In the HPDCP, the PT and PMT are important thermal factors. Especially, the higher the PT is, the more the VSP of the

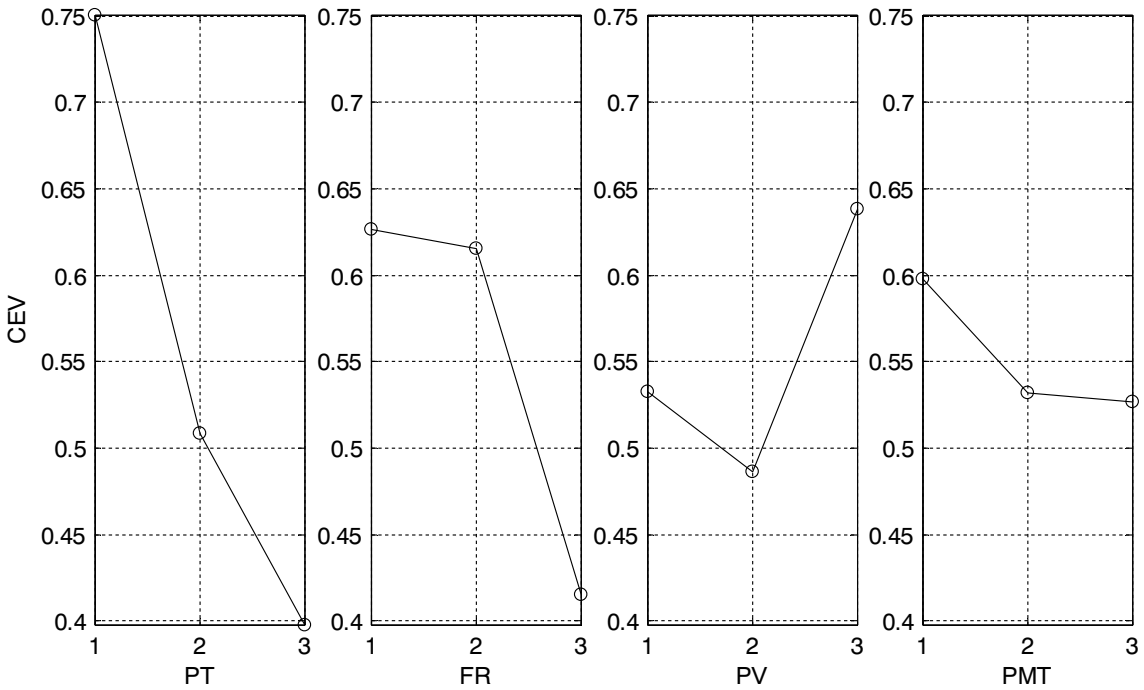

Fig. 3 Mean OQIs of the HPDCP parameters at three levels using combined MADM

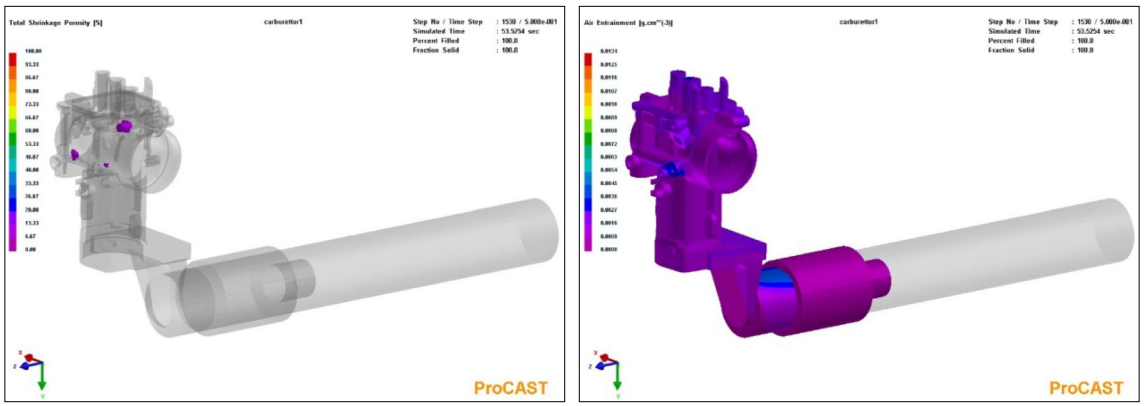

Fig. 4 ProCAST simulation result at the optimal HPDCP parameter values. (left: VSP, right: AE)

casting may increase, the coarser the grain size is, and the die soldering may appear. Oppositely, when the PT is too low, the misrun of the casting may occur. When the PT and PMT are respectively 640 °C, 150 °C in the optimal process, the VSP of the carburetor housing becomes smaller, and the PV of 6.5 m/s ensures the filling rate of molten metal in die cavity. The FR and PT may affect the AE of the carburetor housing. The piston movement at low velocity stage could remove the most of air in the shot sleeve. The higher the PT is, the lower its viscosity is. Moreover, when the FR is too low, the AE may easily occur. When the PT and FR are respectively 640 °C and 40% in the optimal process, the AE becomes smaller. When the die casting could be produced in the air environment, the PT, PMT, FR, and PV may mainly affect the VSP and AE.

We verified that the reasonable PT, FR, PV, 4 and PMT for carburetor housing might, respectively, be 640 °C, 40%, 6.5 m/s, and 150 °C throughout the numerical simulation and practical manufacturing.

To confirm the above-determined optimal HPDCP parameters, we conducted ProCAST simulation at the optimal HPDCP parameter values (PT: 640 °C, FR: 40%, PV: 6.5 m/s, and PMT: 150 °C) and evaluated the VSP and AE. (Fig. 4).

Table 10 OQIs using individual MADMs and combined MADM

	VSP (cm^3)	AE (g/cm^3)	OQIs				Final OQIs
			SAW	TOPSIS	GRA	RSR	Combined MADM
Trial no. 1	0.219505	0.001375	0.791	0.810	0.812	0.800	0.803280
Trial no. 2	0.270404	0.001420	0.665	0.733	0.656	0.700	0.688409
Trial no. 3	0.320834	0.001037	0.665	0.675	0.599	0.620	0.639690
Trial no. 4	0.356488	0.001450	0.465	0.543	0.502	0.360	0.467925
Trial no. 5	0.283652	0.001361	0.653	0.718	0.630	0.660	0.665422
Trial no. 6	0.542853	0.000767	0.252	0.216	0.479	0.360	0.326361
Trial no. 7	0.337115	0.001454	0.507	0.589	0.529	0.420	0.511306
Trial no. 8	0.421927	0.001225	0.386	0.395	0.449	0.360	0.397666
Trial no. 9	0.566143	0.000953	0.146	0.154	0.396	0.260	0.238842
Optimal parameters	0.204878	0.001017	0.927	0.918	0.916	0.960	0.930078

Fig. 5 Carburetor housings made by the optimal HPDCP

The evaluation values of VSP and AE are, respectively, 0.204878 and 0.001017 at the optimal HPDCP parameter values.

Compared with the VST and AE values at 9 experimental trials according to $L_9(3^4)$ in Table 4, the ranks of the VSP and AE at the optimal HPDCP parameters are, respectively, 1 and 3.

To compare the OQI at the optimal HPDCP parameters with the OQIs at 9 experimental trials, we calculated the OQIs using SAW, TOPSIS, GRA and RSR, and final OQIs using combined MADM with the VSPs and AEs at 9 experimental trials and optimal HPDCP parameters as a decision matrix.

Table 10 shows the OQIs at 9 experimental trials and the optimal HPDCP parameters using individual MADMs and combined MADM.

As can be seen in Table 10, the OQIs at the optimal HPDCP parameters were best superior to the OQIs at 9 experimental trials in all the cases of SAW, TOPSIS, GRA, RSR and combined MADM. It demonstrates that the OQI at the optimal HPDCP parameter values has the maximum value compared with the OQIs at 9 experimental trials.

Figure 5 shows the carburetor housings made by the optimal HPDCP. As can be seen in Fig. 5, their appearance

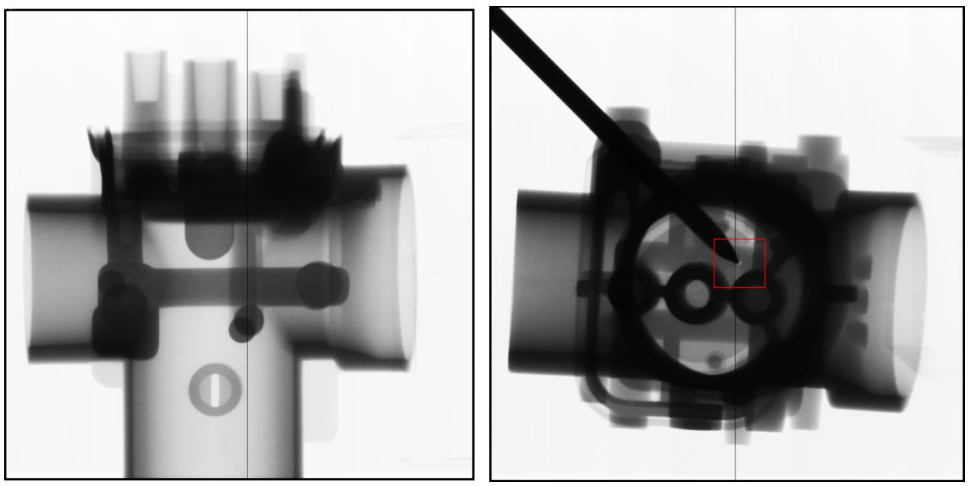

a) b)

Fig. 6 X ray detection of carburetor housing casting: **a** side of casting and **b** upper part of casting

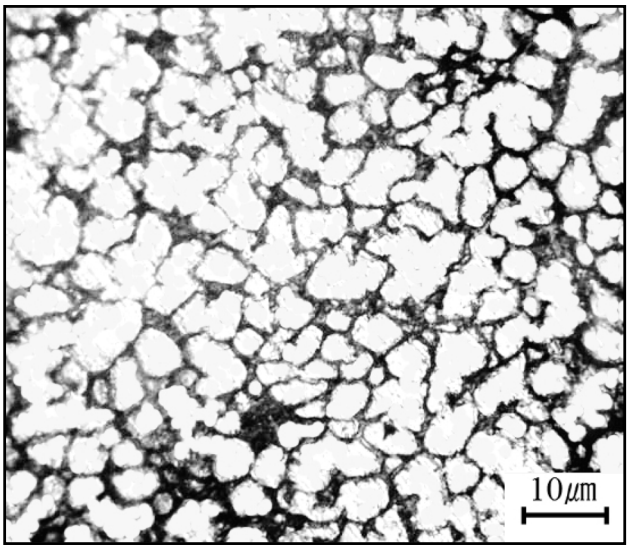

Fig. 7 Microstructure of carburetor housing made by Al alloy

satisfies the requirement of design. Figure 6 shows the X ray detection of the carburetor housing casting.

As can be seen in Fig. 6, the interior of the side of casting (Fig. 6a) does not include any porosity, but the upper part of casting (Fig. 6b) has a bit amount of porosity. It shows that the simulation results agree with the practical HPDCP experiments. Although the carburetor housing casting has a bit amount of porosity in its upper part, it does not leak in a hydraulic test of 0.1 MPa.

Figure 7 shows the microstructure of the carburetor housing made by Al alloy. As can be seen in Fig. 7, the microstructure exhibited a primary α-Al phase (light phase) and eutectic Al-Si phase (dark phase). The primary α-Al phase may be comparatively small and homogeneous. In addition, the Al-Si phase displays a fibrous shape. Moreover, the microstructure of the carburetor housing may be dense and does not identify any shrinkage porosity.

Although there are many influencing factors in the HPDCP, the PT, FR, PV, and PMT may be main factors for improving shrinkage porosity and air entrainment in carburetor housing casting with aluminum alloy. It was verified through our simulation, optimization, and practice.

4 Conclusions

This paper proposed the HPDCP optimization method for improving VSP and AE using Taguchi-based ProCAST simulation and MADM-based overall quality index. By using the method, this paper determined the optimal values of HPDCP parameters such as PT, FR, PV and PMT for improving VSP and AE in the carburetor housing with Al alloy AlSi9Cu1Mg.

As the result, the following conclusions could be drawn:

(1) The optimal values of the HPDCP parameters for improving the VSP and AE were PT of 640 °C, FR of 40%, PV of 6.5 m/s, and PMT of 150 °C, respectively.
(2) The PT was the most effective HPDCP parameter (44.842%) for improving the VSP and AE, and the next was FR (26.867%), PV (19.288%), and PMT (9.003%).

The proposed method could be applied to the HPDCP optimization of the die castings with different sizes and shapes. When the size and shape of the die castings are changed, we should design a 3D pattern and die mold with gating system according to the given size and shape, perform the HPDC simulation using ProCAST according to the Taguchi experimental design, and then determine the optimal HPDCP parameters using MADM and Taguchi method.

The proposed method could be widely applied to not only HPDCP optimization but also other casting process optimization problems. It could be also applied to the other advanced manufacturing process optimization problems. To do this, it needs to select suitable process parameters and quality attributes related to the given manufacturing process, and then determine the optimal manufacturing process parameters by applying the proposed method.

This work did not consider the influences of pouring and feeding systems on the pore defects of castings due to the fixed horizontal cold chamber HPDC machine and die mold. Our future work needs to study this issue.

Acknowledgements This work was supported by Kim Chaek University of Technology, Democratic People's Republic of Korea. The supports are gratefully acknowledged.

Author contribution Ryong-Chol Kim designed the research work, conducted ProCAST simulation experiment for this work, analyzed the result, and wrote the paper. Ji-Yon Yang developed the MATLAB code for determining the optimal HPDCP parameters and wrote the paper. Kyong-Ryul Hong designed the simulation experiment and discussed the result. Won-Chol Yang developed the MATLAB code for calculating the OQIs using MADMs and wrote the paper.

Data availability The authors confirm that the data supporting the findings of this study are available within this article.

Code availability The code that supports the findings of this study is available from the corresponding author (Won-Chol Yang), upon a reasonable request.

Declarations

Ethics approval The authors approve to observe the ethics standard of this journal.

Conflict of interest The authors declare no competing interests.

Open access There is no open access.

References

1. Dou K, Lordan E, Zhang YJ, Jacot A, Fan ZY (2021) A novel approach to optimize mechanical properties for aluminum alloy in high pressure die casting (HPDC) process combining experiment and modelling. J Mater Process Tech 296:117193
2. Hsu QC, Do AT (2013) Minimum porosity formation in pressure die casting by Taguchi method. Mathematical Problems in Engineering 2013:Article ID 920865:1–9
3. Tsoukalas VD (2008) Optimization of porosity formation in AlSi9Cu3 pressure die castings using genetic algorithm analysis. Mater Des 29:2027–2033
4. Brown JR (1999) Foseco Non-ferrous Foundryman's Handbook. In: Brown, J.R. (Ed.). Butterworth-Heinemann, Oxford
5. Neto B, Kroeze C, Hordijk L, Costa C (2008) Modelling the environmental impact of an aluminum pressure die casting plant and options for control. Environ Model Softw 23:147–168
6. Syrcos GP (2003) Die casting process optimization using Taguchi methods. J Mater Process Technol 135:68–74
7. Hu MY, Cai JJ, Sun WL et al (2016) DIE CASTING SIMULATION AND PROCESS OPTIMIZATION OF AN A356 ALUMINUM ALLOY POLISHING PLATE. Int J Metalcast 10(3):315–321
8. Verran GO, Mendes RPK, Valentina LVOD (2008) DOE applied to optimization of aluminum alloy die castings. J Mater Process Technol 2008:120–125
9. Kittur JK, Choudhari MN, Parappagoudar MB (2015) Modeling and multi-response optimization of pressure die casting process using response surface methodology. Intl J Adv Manuf Technol 77:211–224
10. Mohiuddin MVK, A, Hussainy SF, Laxminarayana P, (2016) Influence of process parameters on quality of Al7SiMg alloy casting using statistical techniques. Mater Today: Proceedings 3:3726–3733
11. Apparao KC, Birru AK (2017) QFD-Taguchi based hybrid approach in die casting process optimization. Trans Nonferrous Met Soc China 27:2345–2356
12. Murugarajan A, Raghunayagan P (2019) The impact of pressure die casting process parameters on mechanical properties and its defects of A413 aluminum alloy. Metalurgija 58(1–2):55–58
13. Dou K, Lordan E, Zhang YJ, Jacot A, Fan ZY (2020) A complete computer aided engineering (CAE) modelling and optimization of high pressure die casting (HPDC) process. Journal of Manufacturing Processe; https://doi.org/10.1016/j.jmapro.2020.10.062
14. Yan H, Zhuang W, Yong Hu et al (2007) Numerical simulation of AZ91D alloy automobile plug in pressure die casting process. J Mater Process Technol 187–188:349–353
15. Sharifi P, Jamali J, Sadayappan K, Wood JT (2018) Quantitative experimental study of defects induced by process parameters in the high-pressure die cast process. Metallurgical and Materials Transactions A.49A:3080–3090
16. Boydak O, Savas M, Ekici B (2016) A numerical and an experimental investigation of a high-pressure die-casting aluminum alloy. Int J Metalcast 10(1):56–69
17. Fiorese E, Richiedei D, Bonollo F (2017) Analytical computation and experimental assessment of the effect of the plunger speed on tensile properties in high-pressure die casting. Int J Adv Manuf Technol 91:463–476
18. Armillotta A, Fasoli S, Guarinoni A (2016) Cold flow defects in zinc die casting: prevention criteria using simulation and experimental investigations. Int J Adv Manuf Technol 85:605–622
19. Korti AIN, Abboudi S (2017) Effects of shot sleeve filling on evolution of the free surface and solidification in the high-pressure die casting machine. Int J Metalcast 11(2):223–239
20. Hu MY, Cai JJ, Li N et al (2018) Flow modeling in high-pressure die-casting processes using sph model. Int J Metalcast 12(1):97–105
21. Jiang WM, Fan ZT, Liu DJ, Dong XP, Wu HB, Wang HS (2013) Effects of process parameters on internal quality of castings during novel casting. Mater Manuf Processes 28(1):48–55
22. Jiang WM, Fan ZT, Liu DJ, Wu HB (2013) Influence of gas flowrate on filling ability and internal quality of A356 aluminum alloy castings fabricated using the expendable pattern shell casting with vacuum and low pressure. Int J Adv Manuf Technol 67(9–12):2459–2468
23. Yang JY, Yang WC, Kim RC, Chadha U (2023) Development of overall quality index and overall quality map according to tensile mechanical properties and artificial aging heat treatment conditions for cast aluminum alloy using multi-criteria decision-making and multiple regression model, International Journal on Interactive Design and Manufacturing (IJIDeM); https://doi.org/10.1007/s12008-023-01367-9
24. Yang WC, Yang JY, Kim RC, Om MS, Kim UH, Ri WS, Sok SH (2023) Multi-attribute optimization and influence assessment methodology of casting process parameters combined with integrated MADM and Taguchi method, The International Journal of Advanced Manufacturing Technology; https://doi.org/10.1007/s00170-023-12275-3
25. Yang WC, Kang HS, Ri GS, Kim JS (2022) Consistency improvement method of pairwise matrix based on consistency ratio decreasing rate and attribute weighting method considered decision makers' levels in analytic hierarchy process: application to hip joint prosthesis material selection. Mathematical Problems in Engineering 2022: Article ID 1463006:1–22
26. Yang WC, Choe CM, Kim JS, Om MS, Kim UH (2021) Materials selection method using improved TOPSIS without rank reversal based on linear max-min normalization with absolute maximum and minimum values. Materials Research Express 9: Article ID 065503:1–16
27. Yang WC, Ri W, Yang JY (2022) Choe CM (2022) A new material selection method based on weighted mean values of overall performance scores from different multicriteria decision-making methods, Advances in Materials Science and Engineering. Article ID 4479803:1–9